Electronic Supplementary Material (ESI) for Dalton Transactions.

Supporting Information

Nickel coordination chemistry of bis(dithiocarbazate) Schiff Base ligands; metal and ligand centred redox reactions.

*Jessica K. Bilyj, Nicole V. Silajew and Paul V. Bernhardt**

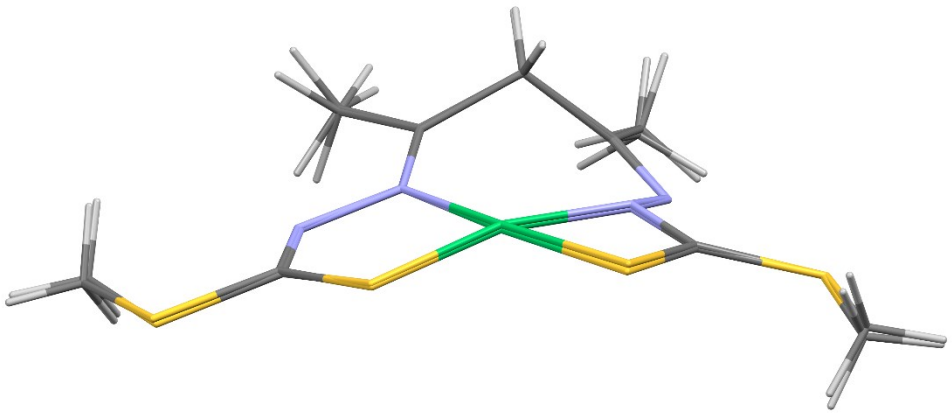

Figure S1. An overlay of the asymmetric units of the polymorphic structures of asym-[Ni(Hacacsme)]. Each structure is shown in capped stick representation in Mercury.

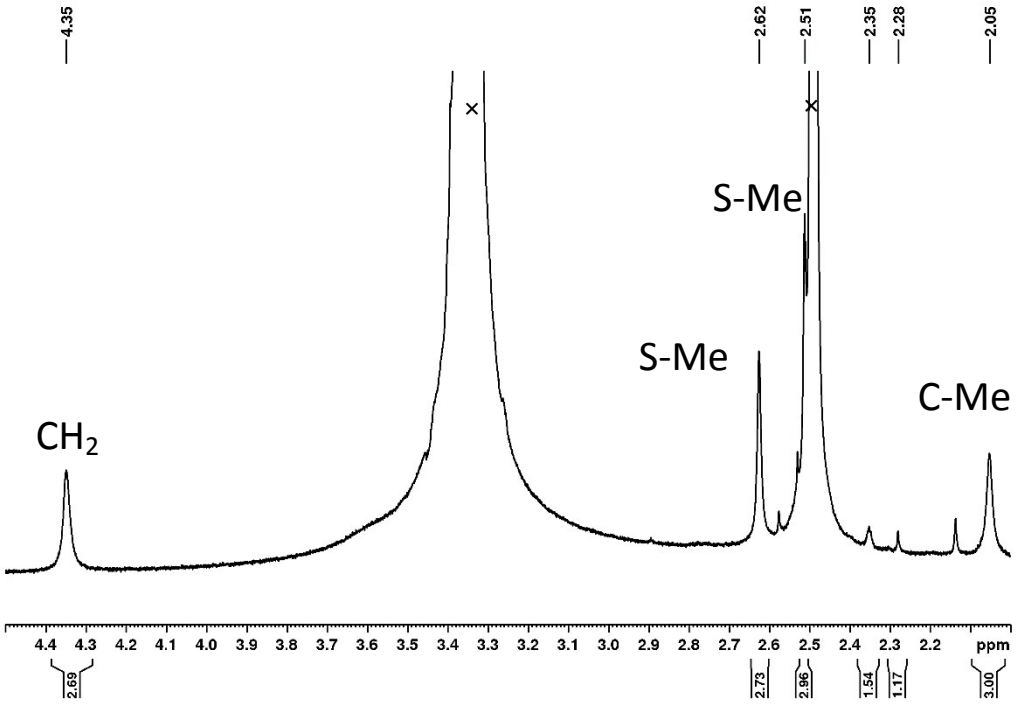

Figure S2. ^{1}H NMR spectrum (DMSO-d_6) of crystalline asym-[Ni(Hacacsme)]. Solvent peaks are indicated with a '×'.

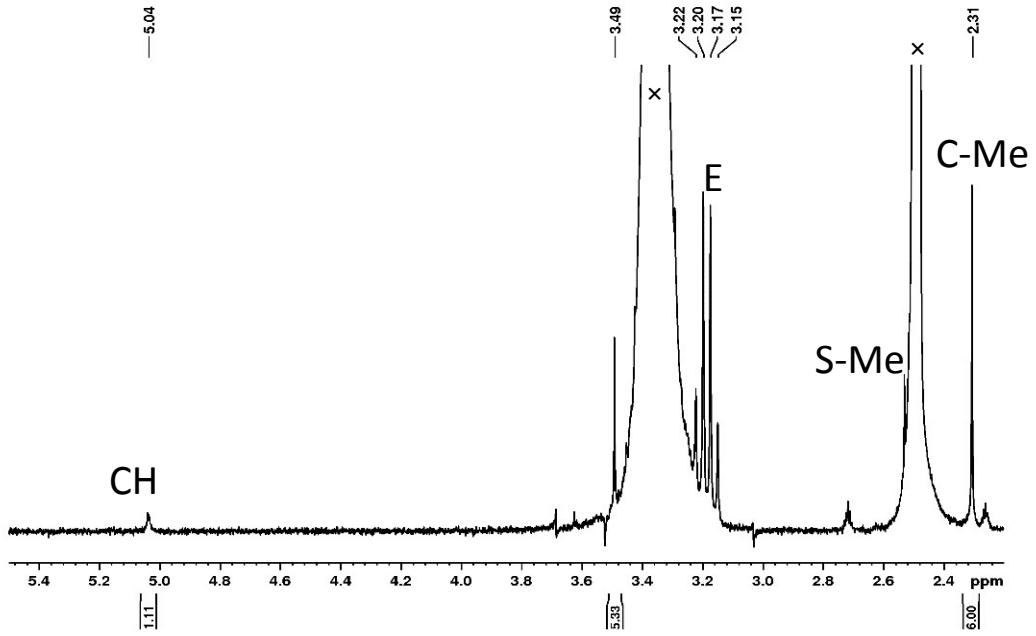

Figure S3. ^{1}H NMR spectrum (DMSO-d_6) of crystalline sym-[Ni(Hacacsme)] (with some Et_4NClO_4 impurity present). Solvent peaks are indicated with a '×', Et_4NClO_4 electrolyte peaks labelled with an 'E'. Peaks from sym-[Ni(Hacacsme)] are highlighted.

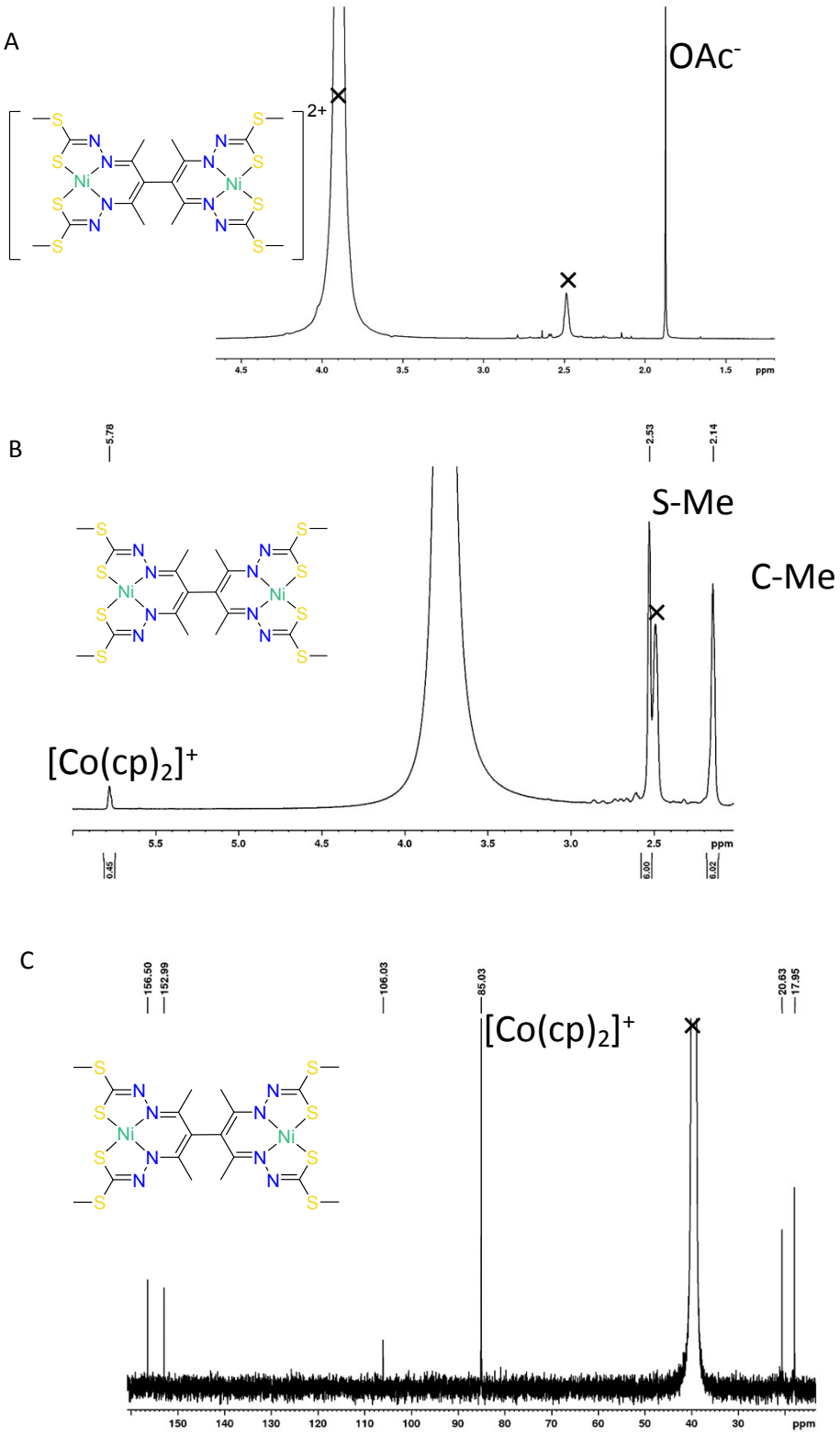

Figure S4. (A) ^{1}H NMR spectrum (DMSO-d_6) of a solution of sym-[Ni(Hacacsme)] after 14 h of oxygenation; (B) ^{1}H NMR after addition of cobaltocene and (C) ^{13}C NMR after addition of cobaltocene. Solvent peaks marked with '×'.

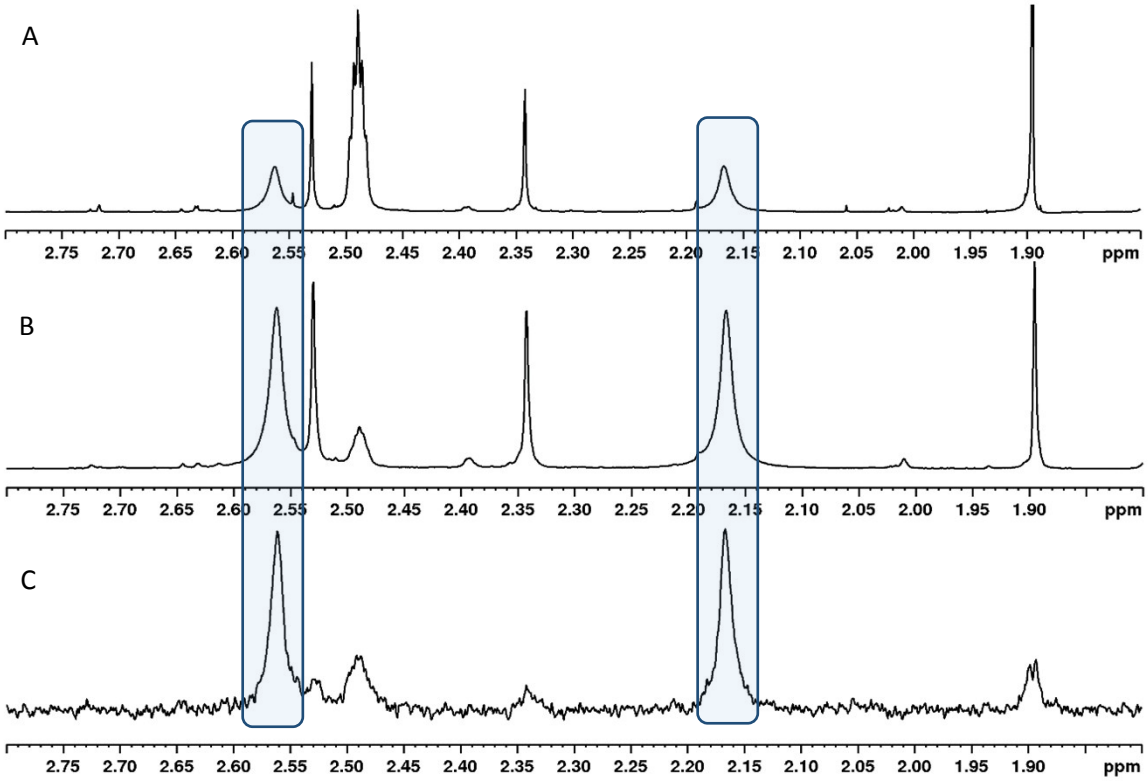

Figure S5. (A) ^{1}H NMR spectrum of sym-[Ni(Hacacsme)] and dimeric sym-[(Ni(Hacacsme))$_2$ in DMSO-d_6 after 3h exposure to oxygen, (B) DOSY NMR spectrum half-suppressed and (C) DOSY NMR spectrum, fully suppressed, showing signals only from sym-[(Ni(acacsme))$_2$] (highlighted).

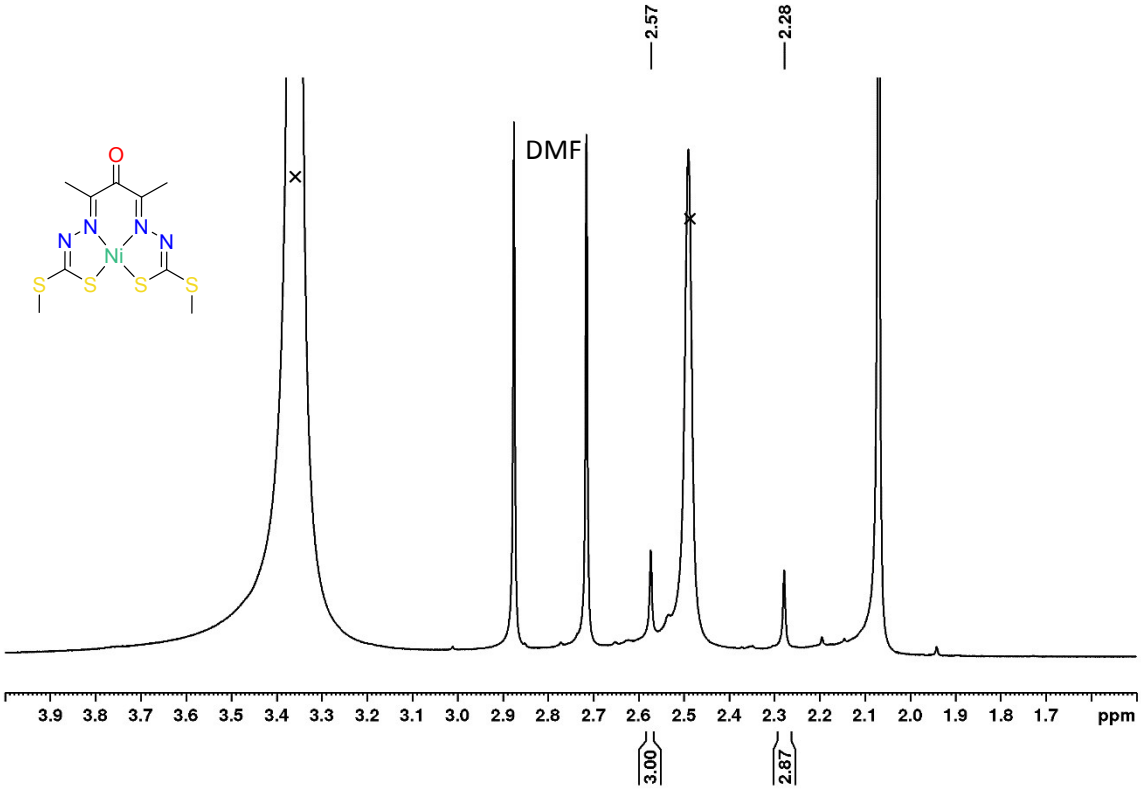

Figure S6. (A) ^{1}H NMR spectrum (DMSO-d_6) of the solid product obtained from oxidation of sym-[Ni(Hacacsme)] in DMF. Peaks from solvent (×) and DMF are indicated.

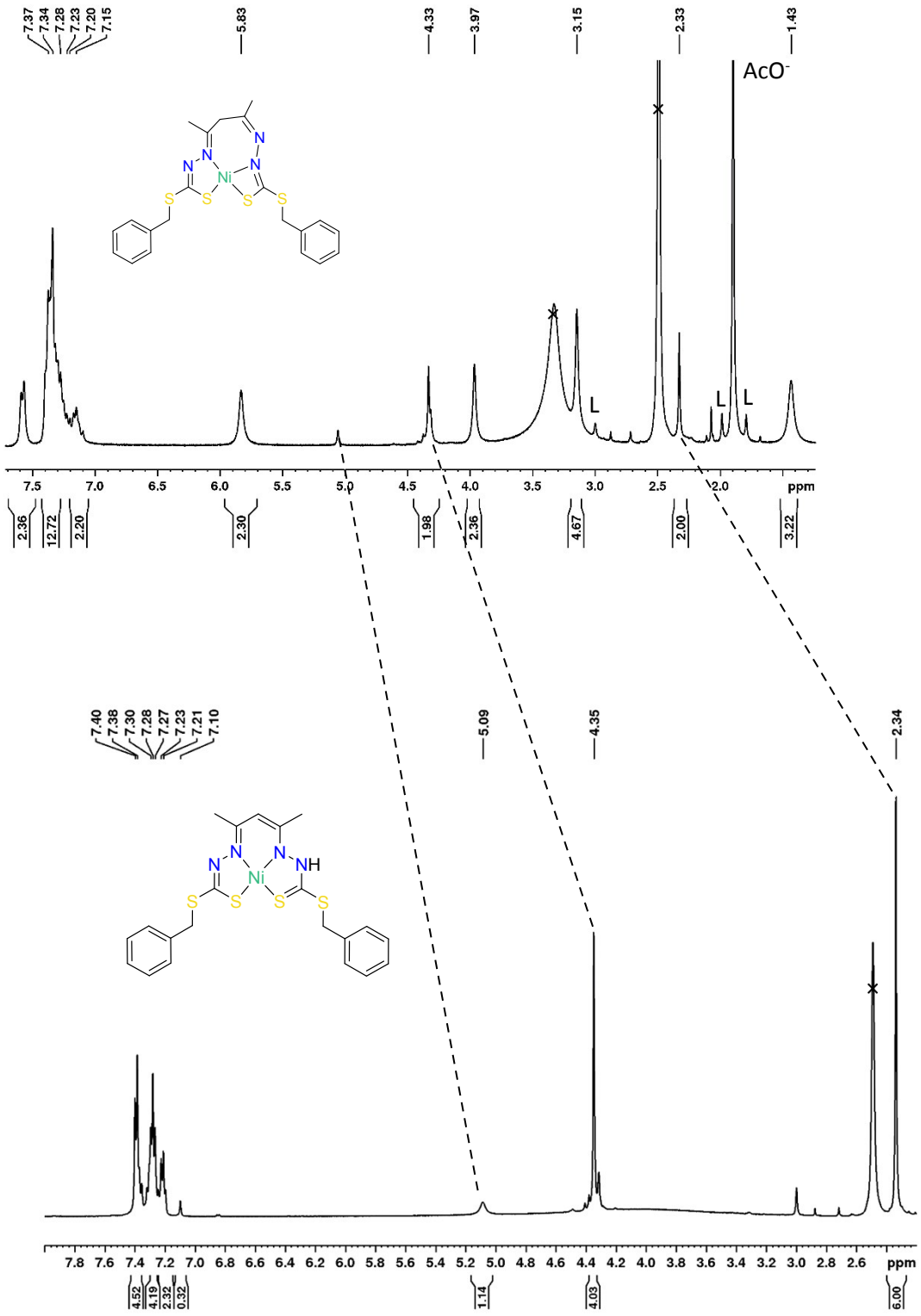

Figure S7. (A) ^{1}H NMR spectrum (DMSO-d_6) of the [Ni(Hacacsbn)] complexation reaction (A) after 30 min and (B) after 90 min. Peaks from solvent (×) and unreacted free ligand (L) are indicated.

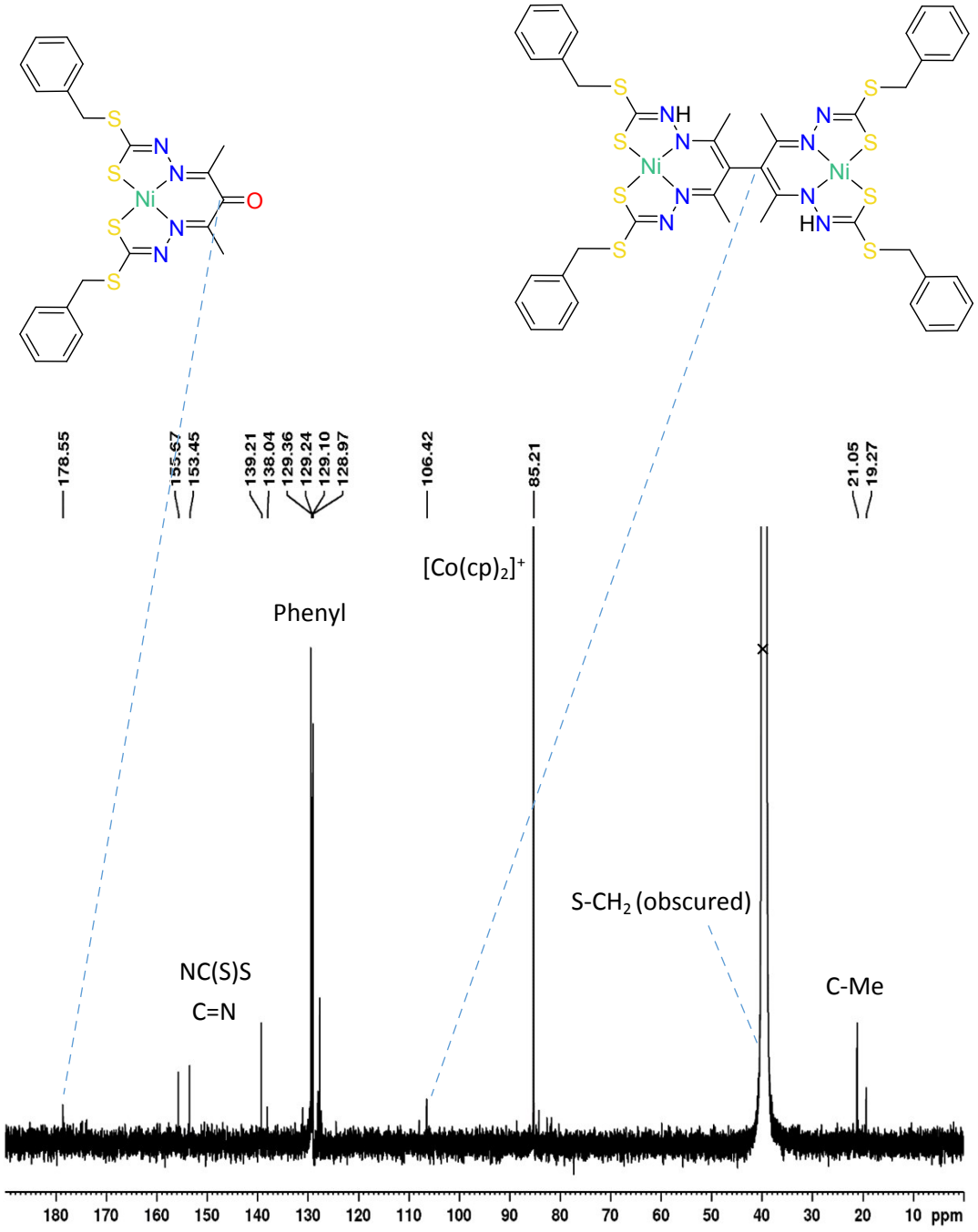

Figure S8. ^{13}C NMR spectrum (DMSO-d_6) of the [Ni(Hacacsbn)] complexation reaction after 24 h oxygenation and treatment with cobaltocene.

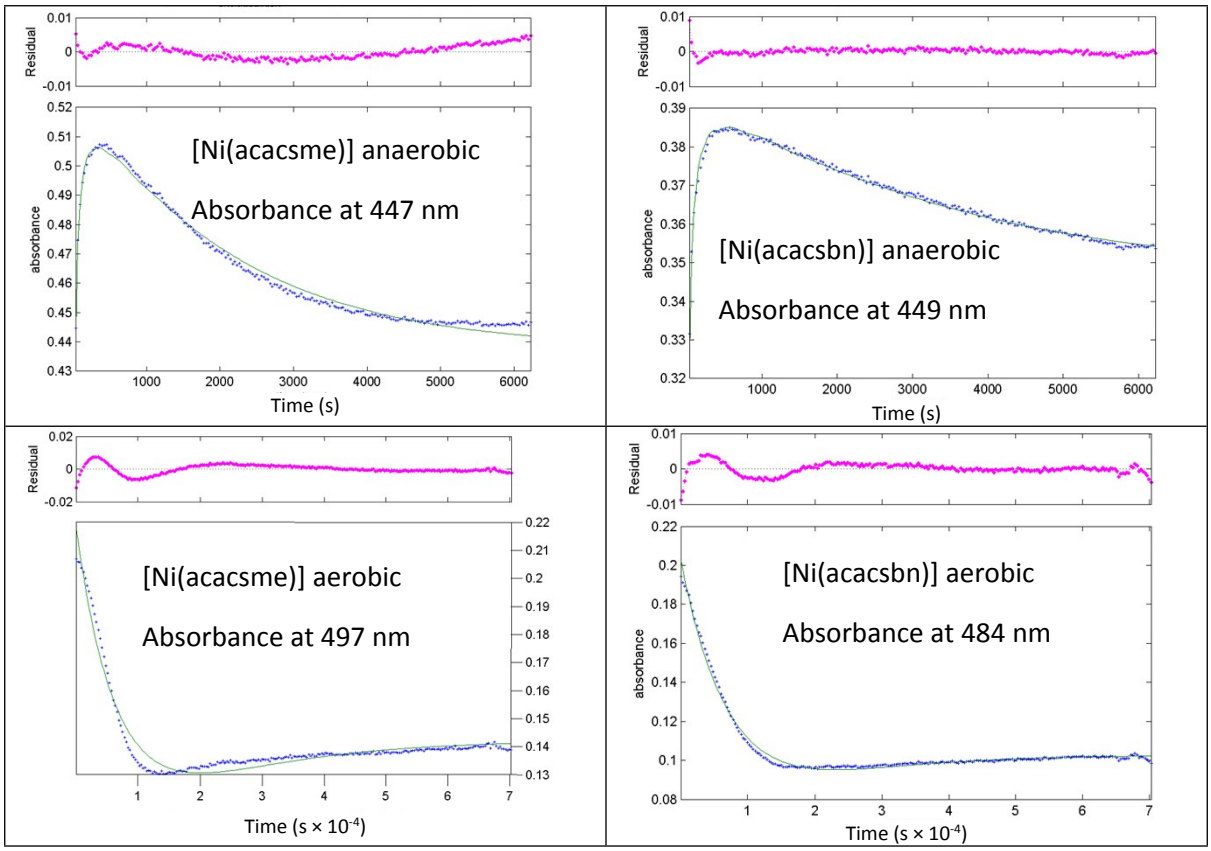

Figure S9. Analysis of the time dependent absorbance changes at selected wavelengths (calculated absorbances are the solid lines using the rate constants in Table 2). The residuals (difference between observed and calculated absorbances) as shown above each plot.

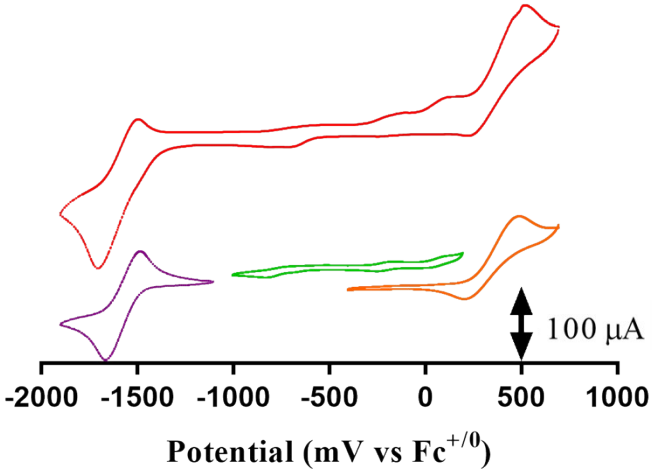

Figure S10. CV of crystalline asym-[Ni^{II}(Hacacsme)] under anaerobic conditions in DMF with 0.1M Et_4NClO_4. Scan rate 200 mV s^{-1}.

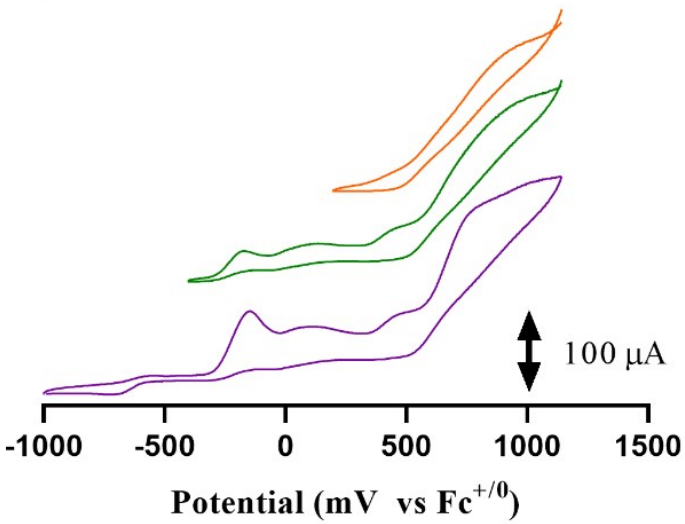

Figure S11. CV of sym-[Ni^{II}(Hacacsme)] after exposure to oxygen for 24 h (DMF with 0.1M Et_4NClO_4, scan rate 200 mV s^{-1})

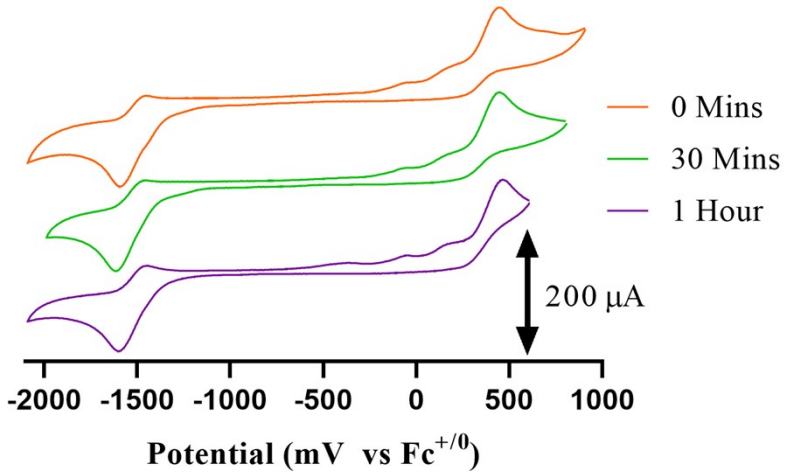

Figure S12. CVs of [Ni^{II}(Hacacsbn)] under anaerobic conditions at different times after complexation (DMF with 0.1M Et_4NClO_4, scan rate 200 mV s^{-1}).

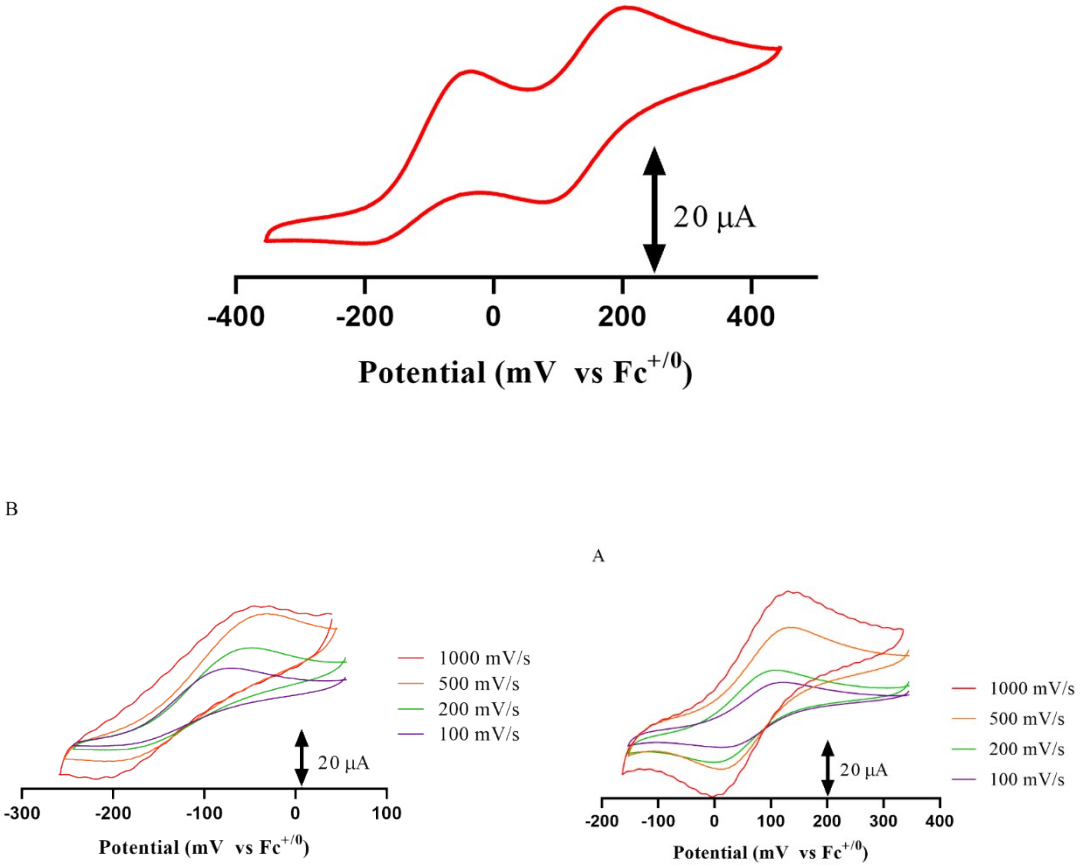

Figure S13. (A) CVs of [Ni^{II}(Hacacsbn)] after exposure to oxygen (DMF with 0.1M Et_4NClO_4, scan rate 200 mV s^{-1}) and (B) scanning the individual couples at different scan rates.

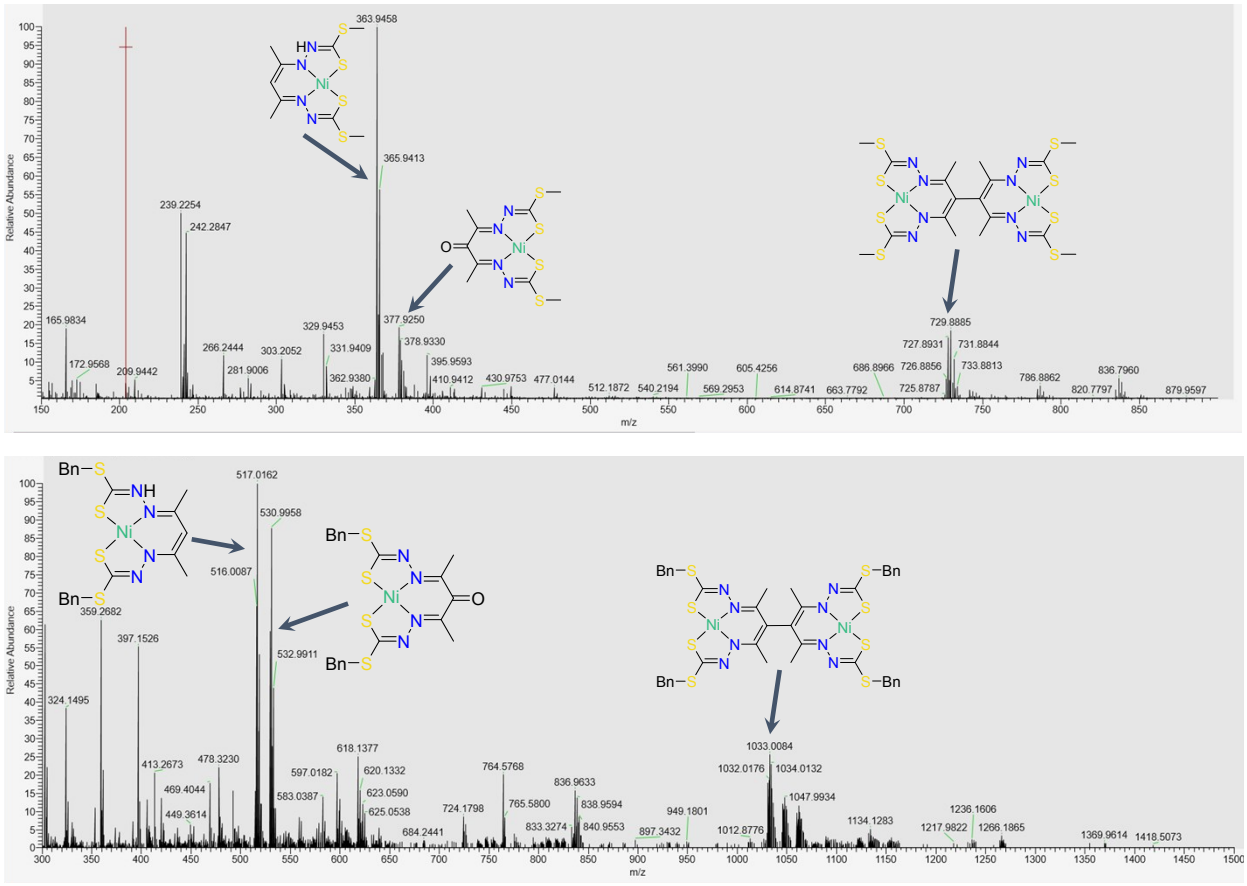

Figure S14. ESI MS of MeCN solutions of (A) [Ni(acacsme)] and (B) [Ni(acacsbn)] after partial aerobic oxidation. Peaks of most relevance are highlighted.

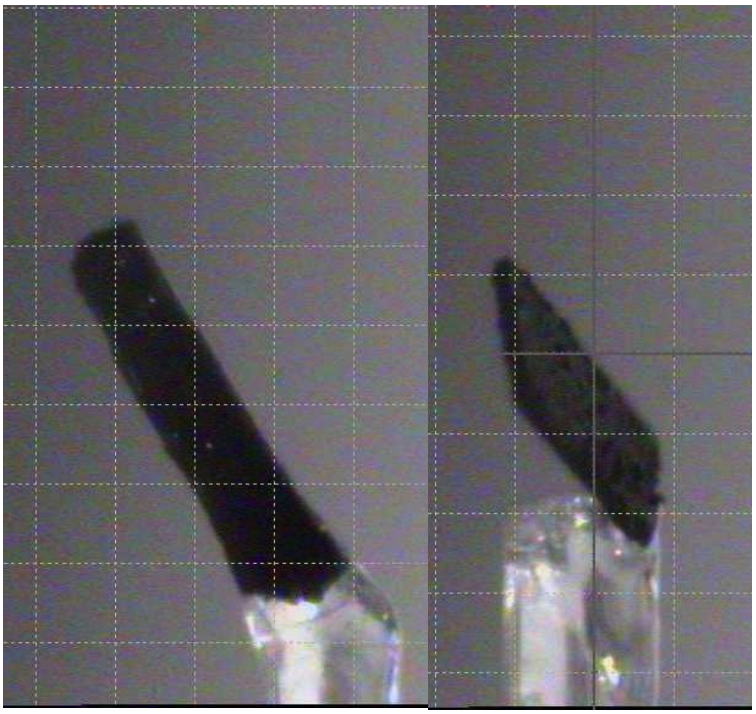

Figure S15. Polymorphic crystals of asym-[Ni(Hacacsme)]. Left is the polymorph crystallising in space group $P2_12_12_1$ with its needle-like appearance and right is the $Pna2_1$ polymorph with its plate-like habit.